

The Discovery of Soft X-ray Loud Broad Absorption Line Quasars

Kajal K. Ghosh¹

and

Brian Punsly²

ABSTRACT

It is been known for more than a decade that BALQSOs (broad absorption line quasars) are highly attenuated in the X-ray regime compared to other quasars, especially in the soft band (< 1 keV). Using X-ray selection techniques we have found “soft X-ray loud” BALQSOs that, by definition, have soft X-ray (0.3 keV) to UV (3000Å) flux density ratios that are higher than typical nonBAL radio quiet quasars. Our sample of 3 sources includes one LoBALQSO (low ionization BALQSO) which are generally considered to be the most highly attenuated in the X-rays. The three QSOs are the only known BALQSOs that have X-ray observations that are consistent with no intrinsic soft X-ray absorption. The existence of a large X-ray luminosity and the hard ionizing continuum that it presents to potential UV absorption gas is in conflict with the ionization states that are conducive to line driving forces within BAL winds (especially for the LoBALs).

Subject headings: (galaxies:) quasars: absorption lines — galaxies: jets — (galaxies:) quasars: general — accretion, accretion disks — black hole physics

1. Introduction

One of the biggest challenges to our understanding of broad absorption line quasars (BALQSOs, hereafter) is how lithium like species (those species producing the resonant UV absorption lines) can form within an out-flowing wind in the presence of the hard ionizing

¹Universities Space Research Association, NASA Marshall Space Flight Center, VP62, Huntsville, AL, USA

²4014 Emerald Street No.116, Torrance CA, USA 90503 and ICRANet, Piazza della Repubblica 10 Pescara 65100, Italy, brian.m.punsly@L-3com.com or brian.punsly@gte.net

continuum of a quasar (EUV and X-ray). Thus, it was no surprise that BALQSOs turned out to be X-ray weak due to thick absorption columns (Green and Mathur 1996). The necessity of this X-ray absorption screen between the central quasar X-ray source and the BAL wind was anticipated by Murray et al (1995). Every deep X-ray observation of a BALQSO has shown significant absorption with the least absorbed sources having neutral hydrogen absorption columns $N_H \gtrsim 10^{22} \text{cm}^{-2}$ and most BALQSOs have absorption columns of $10^{23} \text{cm}^{-2} \leq N_H \leq 10^{25} \text{cm}^{-2}$ (Punsly 2006). As a qualifier, it is possible that the modest radio jet seen in some BALQSOs can also contribute to the X-ray flux and some of these sources might not appear X-ray suppressed due to a secondary source of X-rays from the relativistic jet $\sim 10 - 100$ pc from the central quasar (Brotherton et al. 2005). Thus, we make a distinction between radio quiet (RQBALQSOs), $\log R < 1$, and radio loud BALQSOs (RLBALQSOs), $\log R > 1$, where R is the k-corrected 5 GHz to 2500Å flux density ratio (the RQBALQSOs considered here have $\log R < 0$). The few RQBALQSOs with modest absorption, UM425 and CSO755, $N_H \gtrsim 10^{22} \text{cm}^{-2}$ have fairly typical hard X-ray to UV flux density ratios for radio quiet quasars, but are highly attenuated in the soft X-rays (Aldcroft and Green 2003; Shemmer et al 2006; Murray et al 1995). To this date, all known RQBALQSOs are highly absorbed in the soft X-rays. The lone exception is the X-ray spectrum of IRAS 07598+059 that is consistent with no absorption. However, the X-ray flux relative to the UV is suppressed by a factor of more than 20 compared to a typical radio quiet quasar, thus it is believed that the central quasar X-ray source is completely obscured and we are seeing a secondary weak source, likely the central source seen in reflection off an electron scattering mirror (Imanishi and Terashima 2004).

We have searched the ROSAT database to look for evidence of soft X-ray loud BALQSOs. Previously, the only BALQSO ROSAT detection in the literature is 1245-067 and it is highly absorbed, $N_H \approx 10^{23} \text{cm}^{-2}$ (Green and Mathur 1996). We have found approximately 40 likely detections of BALQSOs by ROSAT and are preparing a catalog of these. However, most of these either are not necessarily strong compared to the UV flux or have poor photon statistics, so it is difficult to determine the X-ray luminosity with much certainty. In sorting through the catalog, we have segregated three AGN that are the most convincing examples of RQBALQSOs that are soft X-ray loud (defined by soft X-ray (0.3 keV) to UV (3000Å) flux density ratios that are higher than typical nonBAL radio quiet quasars), one of which has low ionization UV absorption lines (LoBALQSO). This is even more surprising since the LoBALQSOs require the maximal amount of X-ray screening, otherwise the gas will be over-ionized for the formation of Li-like low ionization species (Murray et al 1995). These BALQSOs could either be intrinsically exceptional objects or objects that are fortuitously configured to reveal some unforeseen physical features of the QSO central engine.

2. The X-ray and UV Data

A search for optical counterparts in the Sloan Digital Sky Survey Data Release 4 of ROSAT PSPC sources from the White-Giommi-Angelini Catalog, White et al. (1994), was performed by Suchkov et al (2006). They found 1744 tentative identifications of ROSAT sources with optical spectra typical of AGN. Our in depth inspection of the SDSS spectra of these 1744 AGNs has identified approximately 44 AGNs as BALQSOs. This section describes the data for the three candidate BALQSOs that are soft X-ray loud, SDSS J023219.52+002106.8, SDSS J101949.75+450256.0 and SDSS J132229.66+141007.3 (corresponding to the WGA counterparts 1WGA J0232.3+0021, 1WGA J1019.7+4502 and 1WGA J1322.4+1410, respectively). Hereafter, the SDSS designations will be abbreviated as 0232, 1019 and 1322.

Event files for the ROSAT PSPC observations of 0232, 1019 and 1322 were retrieved from the ROSAT archive. We use the locally-developed software tool, LEXTRACT, for the extraction of source and background light curves and spectra (Tennant 2006). Good time interval filtering was applied to all the event files. We extracted source counts from circles of $60''$ radius around each source and corresponding backgrounds from nearby source-free regions. Background regions were around 3 to 5 times larger than the source regions. X-ray light curves were binned into 1000 s bins. X-ray spectra of all three sources were binned so that there were at least 30 counts per fitting bin. Spectral redistribution matrices and ancillary response files were retrieved from the ROSAT archive. XSPEC version 11.3 was used to fit the 0.2 – 2.4 keV energy spectra with an absorbed (**phabs**) powerlaw (**powerlaw**) model. Confidence contours in the Γ (photon index)– N_H plane were generated for the models. The confidence contours indicate that $N_H < 2 \times 10^{21} \text{cm}^{-2}$ with $> 99\%$ confidence. The photon statistics are not good enough to segregate out the small intrinsic absorption column density from the Galactic value of N_H . Thus, N_H in of our favored model fit (column 6 of Table 1) is fixed at the Galactic value. We also fitted these spectra with a redshifted, absorbed, powerlaw model. Best fitting model parameters are similar to the previous values. Table 1 describes the details of our fits to the data. The first two columns are the source name and redshift. The next column is X-ray luminosity at the rest frame of the QSOs in the 2-8 keV energy band. Γ is tabulated in columns 4 and 5 based on χ^2 and Cash statistics, respectively. The “goodness of fit” appears in column 7. In the following columns, we define two measures of the X-ray flux density strength relative to the UV: a UV to soft X-ray spectral index defined in terms of the flux density, F_ν as $\alpha_{os} \equiv 0.537 \log[F_\nu(3000\text{\AA})/F_\nu(0.3\text{keV})]$, Laor et al. (1997), and the standard UV to hard X-ray spectral index, $\alpha_{ox} \equiv 0.384 \log[F_\nu(2500\text{\AA})/F_\nu(2.0\text{keV})]$ (Green and Mathur 1996). If there is small nonzero intrinsic absorption as suggested by the confidence contours in the $\Gamma - N_H$ plane, the intrinsic X-ray luminosity is even larger than indicated in column 3 (i.e., α_{os} and α_{ox} are even flatter than in columns (8) and (9)). Thus,

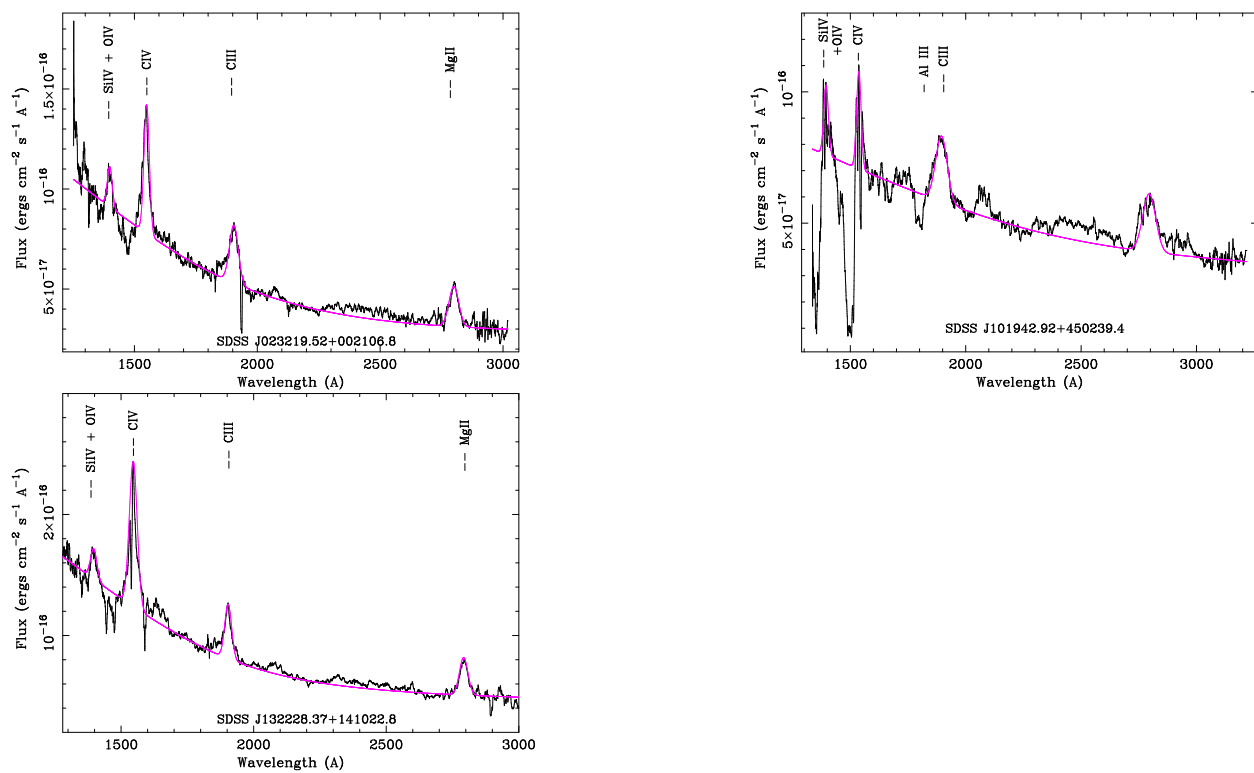


Fig. 1.— The UV spectra from SDSS (from left to right, 0232, 1019, 1322), the best fit continuum is in magenta.

our claims that these sources are soft X-ray loud are conservative. Deeper X-ray observations are required to improve the accuracy of our spectral fits.

The SDSS spectra of the 3 soft X-ray loud RQBALQSOs in the regions of the BALs are presented in Figure 1. The spectra were retrieved from the SDSS database and were analyzed using the *IRAF*¹ software. First, the spectrum was de-reddened using the Galactic extinction curve, Schlegel et al. (1998), then the wavelength scale was transformed from the observed to the source frame. The spectra were fitted in XSPEC with a powerlaw plus multiple gaussian model, including fits for both emission lines and absorption lines (Arnaud 1996). All the model parameters were kept free. The best fit to the SDSS data was determined using χ^2 minimization. If an emission bump around 2500 Å is present then the continuum fit in the CIV (1550 Å) region was extrapolated to longer wavelength. The BALnicity indices quoted in Table 1 are a consequence of the method of spectral fitting described above and other methods might produce different results. However, the exact BALnicity index is not critical to this discussion, the spectra in Figure 1 clearly show BALs and that is the essential point of relevance here. In columns 10 and 11 of Table 1, we compute the BALnicity indices (BIs) for the high ionization CIV trough and the low ionization Al III trough, respectively, per the methods of Weymann et al. (1991); BI > 0 means the source is a BALQSO.

¹IRAF is the Image Reduction and Analysis Facility, written and supported by the IRAF programming group at the National Optical Astronomy Observatories (NOAO) in Tucson, Arizona.

Table 1: X-ray Spectral Models and Balnicity Indices of Soft X-ray Loud BAL Quasars

QSO	z	L_x a	Γ χ^2	Γ Cash	N_H b	χ^2/dof	α_{os}	α_{ox}	BI CIV (km/s)	BI AlIII (km/s)	Type
0232	2.04	0.99 ± 0.17	2.61 ± 0.35	2.55 ± 0.16	2.73	2.2/6	$1.22^{+0.18}_{-0.17}$	$1.35^{+0.03}_{-0.02}$	1626	...	HiBAL
1019	1.87	0.27 ± 0.08	2.89 ± 0.58	2.62 ± 0.18	1.07	0.9/4	$1.33^{+0.30}_{-0.26}$	$1.53^{+0.04}_{-0.02}$	24135	4032	LoBAL
1322	2.05	1.8 ± 0.32	2.62 ± 0.49	3.03 ± 0.20	1.76	3.9/6	$1.16^{+0.25}_{-0.21}$	$1.33^{+0.03}_{-0.02}$	1819	...	HiBAL

^aX-ray luminosity derived from an absorbed powerlaw model in the QSO rest frame from 2.0 -8.0 keV, in units of 10^{45} ergs/s

^bNeutral hydrogen absorption column used in the model in units of 10^{20} cm⁻²

3. Source Identification

Since these objects are so exceptional and the ROSAT error circles are so large, it is important to verify the identifications with the SDSS AGN by Suchkov et al (2006). In Figure 2, we present SDSS “finding charts” for the 3 ROSAT detections. All of the SDSS sources within the 90% confidence source error radius are labeled. Verification of the identifications in Suchkov et al (2006) is predicated on the individual probabilities that each source within the confidence source error radius is not the ROSAT source: the last column in Table 2. In order to arrive at these probabilities, the table first lists the source classification (column 2) for each of the sources in the three ROSAT confidence error radii in Figure 2. The source classifications in Table 2 are based on SDSS photometry using the results of Newberg et al (1999); Strateva et al (2001) and spectra when available. The classifications are amended by the SDSS values of m_B and the VLA/FIRST radio flux densities in the next two columns. This allows a comparison of each putative ROSAT source with the appropriate ROSAT “standard candle” that is identified in column 5. Using the source classification and the hypothesis that each source is the ROSAT detection, each source can be compared individually to the appropriate “standard candle” X-ray properties in columns 6 - 8 in order to assess whether it is a viable identification. The standard candle values are listed on top and the putative source values are listed below in bold and in parenthesis to clearly distinguish the two. For example, consider the F-star that is source 1 in the field of 1WGAJ0232.3+0021 in Figure 2 (row 1 of Table 2). Given the value of M_V associated with its stellar classification and m_V from SDSS photometry, one can determine the distance to the star. If one assumes that this is the ROSAT source then one can compute the intrinsic X-ray luminosity in the ROSAT band, $\log(L_X) = 34.20 \pm 0.20$ which is much larger than any of the ROSAT F stars of similar M_V in Suchkov et al (2003), $\log(L_X) = 29.38 \pm 0.50$. If the Suchkov et al (2003) data fits a log normal distribution then we can rule out the F-star as the ROSAT source with > 0.9999 probability. If however, the tail of the probability distribution for $\log(L_X)$ of ROSAT F-stars beyond 3σ , does not obey Gaussian statistics (i.e., there are extra outliers in the tail), the F-star can not be ruled out categorically. The M-stars are treated in a similar manner using the “standard candle” $\log(L_X)$ values for M-stars of matched M_V from Marino et al. (2000).

Similarly, there is a standard candle for each field galaxy in Figure 3 that is determined by the galaxy type, the 1.4 GHz flux density and m_B . The X-ray fluxes of radio quiet galaxy standard candles are given by Refreiger et al. (1998). These standard candle fluxes are compared to the observed ROSAT fluxes in the 1WGA fields in column 6. The ROSAT fluxes in the 1WGA fields are three orders of magnitude too large to be consistent radio quiet galaxy counterparts. The quasar soft X-ray properties have been studied in Laor et al. (1997) by means of α_{os} . The quasar values of α_{os} are compared to the Laor et al. (1997)

Table 2: Probability of False Identification of the Sources in the 1WGA Fields

Source	Type	m_B	1.4 GHz (mJy) ^a	Standard Candle	Flux ^b	Standard Candle (Putative Source) Log L_x ^c	α_{OS} ^d	Prob. False ID
1WGAJ0232.3+0021								
source 1	FV7-9 star	16 ± 0.03	< 0.99	ROSAT F stars, $3.0 < M_V < 4.0$...	29.38 ± 0.5 (34.20 \pm 0.20)	...	> 0.9999
source 2	spiral galaxy	20.8 ± 0.1	< 0.99	radio quiet spirals	4.4 ± 0.7 (6592)	> 0.9999
source 3	quasar ^e $z = 0.768$	22.0 ± 0.15	< 0.99	radio quiet unobscured quasar	1.52 ± 0.26 (0.56^{+0.14}_{-0.13})	> 0.9999
source 4	BALQSO	19.4 ± 0.05	< 0.99	radio quiet quasar	1.52 ± 0.26 (1.22^{+0.18}_{-0.17})	0.8289
1WGAJ1019.7+4502								
source 1	M3.5 - M4.5 star	20.7 ± 0.1	< 0.98	ROSAT M3.5 - M4.5 stars	...	27.72 ± 1.05 (31.15 \pm 0.54)	...	0.9982
source 2	spiral galaxy	22.9 ± 0.3	< 0.98	radio quiet spirals	0.63 ± 0.7 (3217)	> 0.9999
source 3	M4.5 - M5.5 star	17.6 ± 0.03	< 0.98	ROSAT M4.5 - M5.5 stars	...	26.96 ± 0.61 (29.84 \pm 0.10)	...	> 0.9999
source 4	spiral galaxy	21.3 ± 0.1	< 0.98	radio quiet spirals	2.8 ± 0.7 (3217)	> 0.9999
source 5	elliptical galaxy	22.7 ± 0.25	< 0.98	radio quiet ellipticals	3.1 ± 0.7 (3217)	> 0.9999
source 6	BALQSO	19.3 ± 0.05	< 0.98	radio quiet quasar	1.52 ± 0.26 (1.33^{+0.30}_{-0.26})	0.7675
1WGAJ1322.4+1410								
source 1	FV8-9 star	19.4 ± 0.05	< 0.91	ROSAT F stars, $3.0 < M_V < 4.0$...	29.38 ± 0.5 (34.11 \pm 0.20)	...	> 0.9999
source 2	FV6-7 star	20.6 ± 0.1	< 0.91	ROSAT F stars, $3.0 < M_V < 4.0$...	29.38 ± 0.5 (34.76 \pm 0.53)	...	> 0.9999
source 3	spiral galaxy	21.3 ± 0.1	< 0.91	radio quiet spirals	3.8 ± 0.7 (12046)	> 0.9999
source 4	elliptical galaxy	22.6 ± 0.2	< 0.91	radio quiet ellipticals	3.1 ± 0.7 (12046)	> 0.9999
source 5	BALQSO	18.4 ± 0.03	< 0.91	radio quiet quasar	1.52 ± 0.26 (1.16^{+0.25}_{-0.21})	0.8413

^a Upper limit on flux density from VLA/FIRST

^b X-ray flux in the observers frame 0.2 - 2.4 keV (10^{-17} ergs/s cm^{-2})

^c Putative source luminosity is computed from χ^2 fit to ROSAT data in figure 1

^d α_{OS} is defined in Laor et al. (1997) and the characteristic quasar range of values is from that paper

^e This is not an obscured (red quasar) based on SDSS colors and 2MASS upper limit on flux density that yields, $R - K < -0.8$. The photometric redshift is based on SDSS colors

characteristic quasar values in column (8). The only objects in Table 2 without a high statistical significance for not being the ROSAT detection are the BALQSOs.

There is still the possibility that the 1WGA sources are interlopers, i.e. it was anomalously bright during the PSPC observations and then faded subsequently. The WGACAT catalog contains more than 68000 sources and a total of 216 variable sources detected that could be considered interlopers (White et al. 1994). Thus, the chance of finding an interloper in one of these 3 fields is < 0.0095 .

4. Discussion

In this Letter, we describe 3 BALQSOs that have soft X-ray to UV ratios that are larger than typical quasars (see the α_{os} values in Table 2). Hence, the designation as soft X-ray loud. However, the α_{ox} values are not exceptional for quasars due to the steep X-ray spectral indices (Strateva et al 2005). These are also the first known BALQSOs with X-ray absorption consistent with pure Galactic absorption. The tentative discovery of soft X-ray loud BALQSOs is completely unexpected based on theoretical treatments of BALQSOs. The conundrum posed by this new class of AGN is how can a BAL region coexist with a powerful source of X-rays, since even a modest flux of X-rays will over-ionize the gas making it impossible to form Li-like atoms Murray et al (1995). On a speculative note, a relativistic X-ray jet beamed towards earth and away from the BAL gas is a possibility (Punsly 1999a,b). It is now known that there are BALQSOs with relativistic jets beamed toward earth and a jet similar to the one in Figure 1 of Ghosh and Punsly (2007) that is radio weak, but X-ray strong would conform to the properties of the BALQSOs in Tables 1 and 2. There are extragalactic jets that have X-ray and radio properties in-line with theses sources. Extreme high frequency peaked BL Lac objects such as PG1553+113, at $z \approx 2$, would have an apparent X-ray luminosity of $\gtrsim 10^{45}$ ergs/s, a steep X-ray spectrum and would have a radio flux at 1.4 GHz of about 0.1 - 0.5 mJy in agreement with the properties of the BALQSOs presented here (Osterman et al 2006).

REFERENCES

- Aldcroft, T.L., Green, P.J., 2003 ApJ **592** 710
- Arnaud, K.A., 1996, **Astronomical Data Analysis Software and Systems V**, eds. Jacoby G. and Barnes J., ASP Conf. Series volume 101, p17
- Brotherton, M. et al 2005, AJ textbf130 2006

- Ghosh, K. and Punsly, B. 2007 ApJL **661** 139
- Green, P. and Mathur, S. 1996 ApJ **462** 637
- Imanishi, M. and Terashima, Y., 2004 AJ **127** 758
- Laor, A. et al 1997, ApJ **477** 93
- Marino, A.; Micela, G.; Peres, G. 2000, A& A, **353**, 177.
- Murray, N. et al 1995, ApJ **451** 498
- Newberg, H. J., Richards, G., Richmond, M., Fan, X. 1999, ApJS **123** 377
- Osterman, M. A. et al 1999, AJ **132** 837
- Punsly, B. 1999, ApJ **527** 609
- Punsly, B. 1999, ApJ **527** 624
- Punsly, B. 2006, ApJ **647** 886
- Refregier, A., Helfand, D., McMahon, R. 1997, ApJ **478** 476
- Schlegel, D. J., Finkbeiner, D. P. & Davis, M. 1998, ApJ **500** 525
- Shemmer, O. et al (2005) AJ **130** 2522
- Strateva, I. et al (2001) AJ **122** 1861
- Strateva, I. et al (2005) AJ **130** 387
- Suchkov, A. A., Makarov, V. V. & Voges, W. (2003) ApJ **595** 1206
- Suchkov, A, Hanisch, R., Voges, W., Heckman, T. (2006) AJ **132** 1475
- Tennant, A(2006) AJ **132** 1372
- Weymann, R.J., Morris, S.L., Foltz, C.B., Hewett, P.C. 1991, ApJ **373**, 23
- White N.E., Giommi P. & Angelini L. 1994,<http://wgacat.gsfc.nasa.gov/wgacat/wgacat.html>

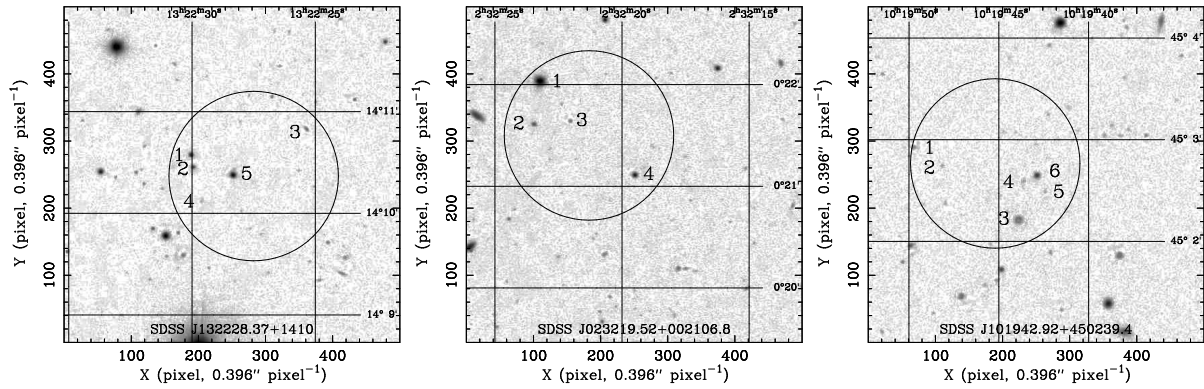


Fig. 2.— Finding charts for the 3 ROSAT detections, from left to right, 0232, 1019 and 1322. The SDSS identification from Suchkov et al (2006) is at the center of each frame. The circles represent the 90% ROSAT confidence source error radius.